IFAI Geosynthetics Conference
Feb. 10-13, 2019 | Houston, TX USA

Investigation of Combined Effects on Measured Strains of Geogrid

Seyed Mustapha Rahmaninezhad[1], Jie Han[2], Wessam Mohammed[3], and Ghaith Abdulrasool[4]

[1] Graduate Research Assistant, Department of Civil, Environmental, and Architectural Engineering, the University of Kansas, 1530 W. 15th St., Lawrence, KS 66045-7609, USA; e-mail: rahmaninezhad@ku.edu
[2] Glenn L. Parker Professor of Geotechnical Engineering, Department of Civil, Environmental, and Architectural Engineering, the University of Kansas, 1530 W. 15th St., Lawrence, KS 66045-7609, USA; e-mail: jiehan@ku.edu
[3] Ph.D. Student, Department of Civil, Environmental Engineering, Villanova University, Villanova, PA 19085, USA; e-mail: wmohamme@villanova.edu
[4] Iraqi Ministry of Oil, Design Division, Baghdad, Iraq; e-mail: m.sghaith@yahoo.com

ABSTRACT

Geosynthetics have been commonly used for soil stabilization/reinforcement in roads, slopes, and walls. To determine tension in the geosynthetic, strain gauges are often attached on the geosynthetic. In many studies, foil electrical resistance strain gauges have been attached on one side of the geosynthetics to measure their strains. Such attachment of strain gauges is acceptable if only pure tension develops in the geosynthetics. However, in some applications, such as geosynthetic-reinforced column-supported (GRCS) embankments and geosynthetic-reinforced retaining (GRR) walls, the geosynthetic is subjected to bending and friction in addition to tension. Bending and friction may happen locally during construction, especially around aggregates. To address this issue, two strain gauges attached on the upper and lower sides of the geosynthetic at the same location have been suggested and used in the practice. This experimental study investigated the combined effects of tension, bending, and friction on the measured strains on the upper and lower sides of uniaxial geogrid specimens. The specimens were instrumented with resistance strain gauges and subjected to tension, bending, and friction at the same time, which were simulated by wrapping the specimen around three cylinders of different diameters. The test results show the combination of tension, bending, and friction reduced the average value of the upper and lower strains by 28% as compared with the tension only. The cylinder diameter did not have any effect on the measured strains of the geogrid on the cylinder.

INTRODUCTION

Geosynthetics have been commonly used for soil stabilization/reinforcement in roads, slopes, and walls. To understand the geosynthetic behavior, determine its actual tension, and evaluate its long-term performance, strains on geosynthetics have been measured in the field (e.g., Fannin and Hermann 1990; Perkins and Lapeyre 1997; Bathurst et al. 2002; Hirakawa et al. 2003; Leshchinsky et al. 2010; Warren et al. 2010, Jiang et al. 2016). Three types of extensometer

instruments have been used to measure strains on geosynthetics, which can be categorized into (ASTM D-4595-11, 2011): (1) direct reading extensometers (e.g., foil resistance strain gages); (2) semi-remote reading extensometers (e.g., wires, pulley, and tell-tale system); and (3) remote extensometers (e.g., optical instruments).

These instruments are used to measure global and local strains across the geosynthetic. The global strain can be determined by instruments (e.g., pairs of extensometers) that are capable to measure the change of the distance between two reference points on the geosynthetics. Therefore, the global strain is an average strain along a length that is much larger than the common length of foil resistance strain gages (SGs). In the case of a geogrid, the global strain represents the strain along one or more aperture lengths (Bathurst et al. 2002). However, the local strain is referred to the strain recorded by a gauge at the point of attachment.

The flexible nature, shape, and polymer type of geosynthetics and the soil-geosynthetic interaction in different applications may not allow the use of all types of extensometer instruments (Warren et al. 2010). The foil resistance strain gauges are the most common type of strain gauges that consist of one insulating flexible backing supporting a metallic foil pattern. ASTM D-4595-11 (2011) suggested the use of SGs to find the tensile properties of geotextiles by the wide-width method. Moreover, the literature shows many laboratory and field studies used foil resistance strain gages on geosynthetics (Rahmaninezhad et al. 2018).

In many studies, SGs were attached just on one side of geosynthetic elements to measure their tensile strains. However, in some cases, the measured strains from one side of the geosynthetic element might be affected by bending. In some structures, such as geosynthetic-reinforced column-supported (GRCS) embankments and geosynthetic-reinforced shallow foundations, the geosynthetic sheets could be subjected to differential settlement (Wayne et al. 1998; Han and Gabr, 2002; Rahmaninezhad et al. 2009; Yasrobi et al. 2009; Huang and Han 2010). In these cases, the geosynthetic elements were bent and the measured strains might be affected by bending (Perkins and Lapeyre 1997; Raymond 2002; Maheshwari and Viladkar 2009; Rahmaninezhad et al. 2016; Weldu et al. 2016; Rahmaninezhad et al. 2018). Therefore, some researchers attached two SGs on both sides of the geosynthetics to eliminate the bending effect. However, on the top of columns, the geosynthetic is subjected to a combination of tension, bending, and friction. Whether this technique of using strains on two sides of the geosynthetic could successfully simulate the combined effect has not been well investigated.

The objective of this study is to evaluate the combined effects of tension, bending, and friction on the measured strains on the geosynthetic and the relationship between local and global strains. Bending and friction of a geogrid were simulated by wrapping the geogrid specimens around three cylinders of different diameters.

EXPERIMENTAL TESTS

Test Apparatus. Figure 1 shows the setup of the tensile test of a geogrid specimen. The ASTM D6637 standard (ASTM, 2015) for measuring tensile strength of a geogrid was adopted for this study. Bending and friction on a geogrid were simulated by wrapping the geogrid specimen around a cylindrical pipe. Three cylindrical pipes were used and had nominal outside diameters of approximately 65, 100, and 160 mm. One end of the geogrid was connected to the frame using a metal bar clamp like a bodkin connector. Another end of the geogrid was connected to a load cell. Loads were applied by placing weights in a bucket hanging under one end of the geogrid. One load cell was used to measure the actual load.

Geogrid. One type of uniaxial (UX) HDPE geogrid was used in this study. The physical and mechanical properties of the geogrid provided by the manufacturer are shown in Table 1. To avoid possible property variability of different ribs, only one rib was used for loading and measurements.

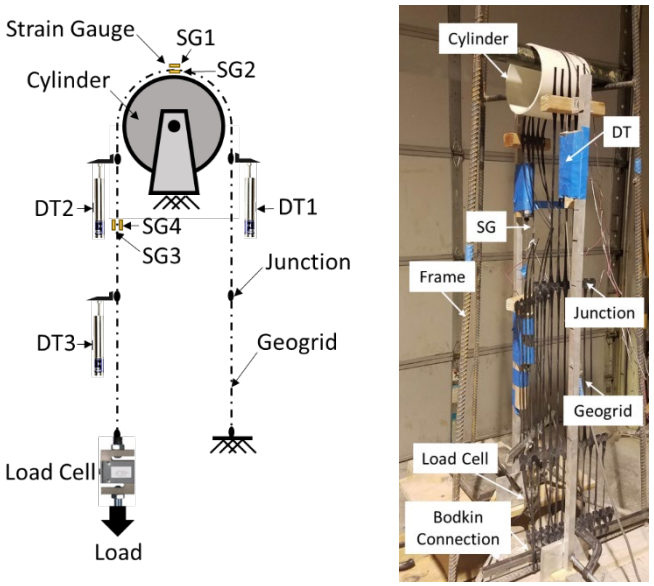

(a) **(b)**

Figure 1. Test Setup: (a) schematic cross-section and (b) picture of the test setup.

Table 1. Properties of geogrids (provided by the manufacturer).

Geogrid Properties	
Tensile Strength @ 5% Strain (kN/m)	27.0
Ultimate Tensile Strength (kN/m)	58.0
Junction Strength (kN/m)	54.0
Flexural Stiffness (mg-cm)	500,000
Minimum Reduction Factor for Installation Damage (RF_{ID})	1.05
Reduction Factor for Creep for 120 yr design life (RF_{CR})	2.60
Minimum Reduction Factor for Durability (RF_{D})	1.00

Measurements. The applied load was measured using an S-shape load cell with a capacity of 10 kN. The elongations of the rib of the geogrid at two locations were measured using three displacement transducers (DTs) with a displacement limit of 50 mm. The global strains were calculated using the elongations in the ribs of the geogrid measured by DTs. Furthermore, the geogrid was instrumented with four SGs: SG1, SG2, SG3, and SG4, as shown in Figure 1. The SGs were attached on both sides of the geogrid rib in the middle of the aperture (Figure 2). The strain gauges had a gauge length of 5 mm and a resistance of 120 Ω. The measured strains from these SGs represent the local strains.

(a) **(b)**

Figure 2. (a) Location of SG on the middle of the geogrid rib and (b) arrangement of the geogrid and SGs on one cylinder.

RESULTS AND DISCUSSION

Global Strain. Figure 3 shows the relationships of the applied load versus the global strain of the geogrids. The rib with DT2 and DT3 was under tension only. Therefore, the slope of the trend-line for the rib with DT2 and DT3 represents the tensile stiffness of the geogrids. With different cylinder diameters, the tensile stiffness of the rib was similar (i.e., 12-13 kN/rib). However, the global strains calculated from DT1 and DT2 were affected by the combination of tension, bending, and friction. The results show that at the same applied load, the global strain in the rib induced by tension only was higher than the one induced by tension, bending, and friction. In addition, Figure 3 shows that at the same global strain, the load carried by the geogrid rib induced by tension only was less than that induced by tension, bending, and friction because the friction was in the opposite direction to the tension and additional load was required to overcome the friction to induce the same strain on the geosynthetic. For example in Figure 3(a), at the global strains of 0.5%, 1%, and 1.5%, the differences between the loads carried by the geogrid rib under tension only and the rib under tension, bending, and friction were approximately 0.03, 0.04, 0.03 kN, respectively. Since bending does not induce any tensile resistance, this difference is the load carried by friction between the geogrid and the cylinder. The average loads carried by friction on the cylinders with diameters of 65, 100, and 160 mm were approximately 0.025, 0.020, and 0.016 kN, respectively, from the beginning to the end of the tests.

Global Strain and Average Local Strain. The correlation factor, CF, is the ratio of the measured global strain by the displacement transducers to the local strain by the strain gauge. The CF can be estimated using the following equation:

$$CF = \frac{Global\ Strain}{Local\ Strain} \qquad \text{Eq. (1)}$$

Figure 4 shows the relationship of the global strain versus the average local strain of the geogrids. The average local strain represents the average of the measured strains from SGs attached on the upper and lower sides of the geogrid and can be estimated using the following equation:

$$Average\ Local\ Strain = \frac{\varepsilon_{upper} + \varepsilon_{lower}}{2} \qquad \text{Eq. (2)}$$

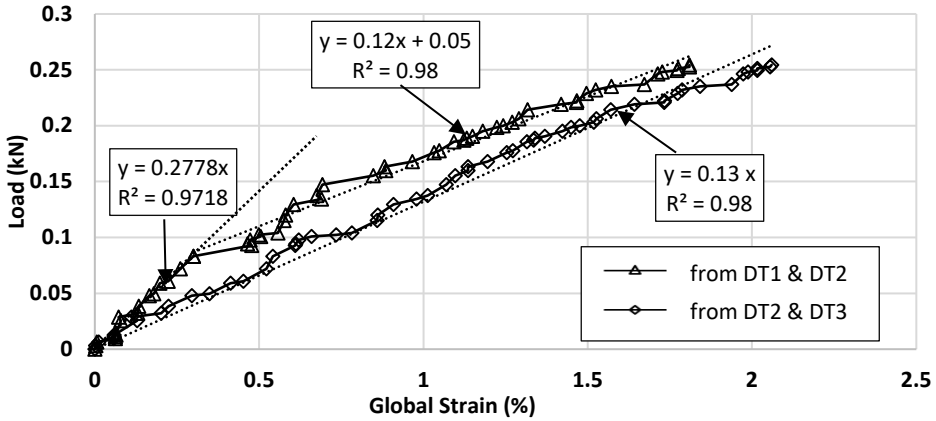

(a)

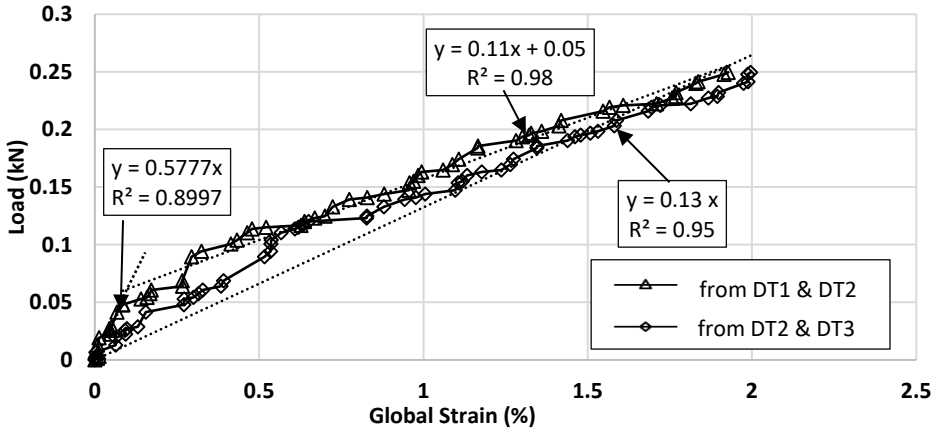

(b)

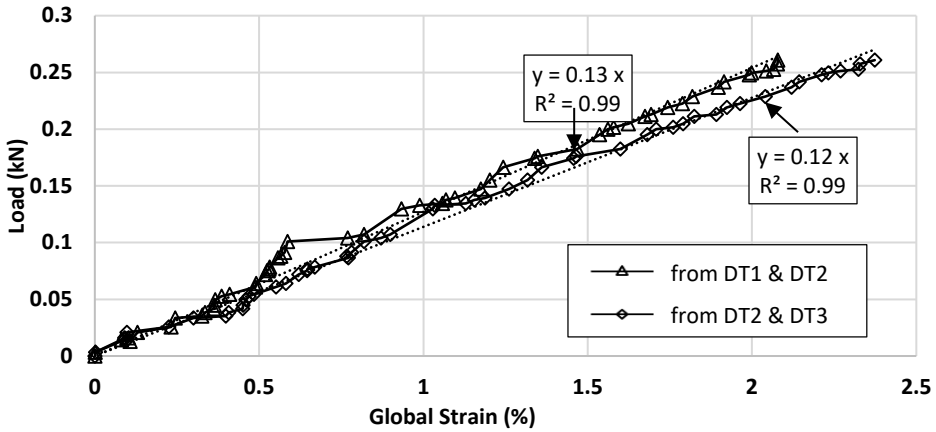

(c)

Figure 3. Applied load versus global strain with the cylinder diameter of: (a) 65 mm; (b) 100 mm; and (c) 160 mm.

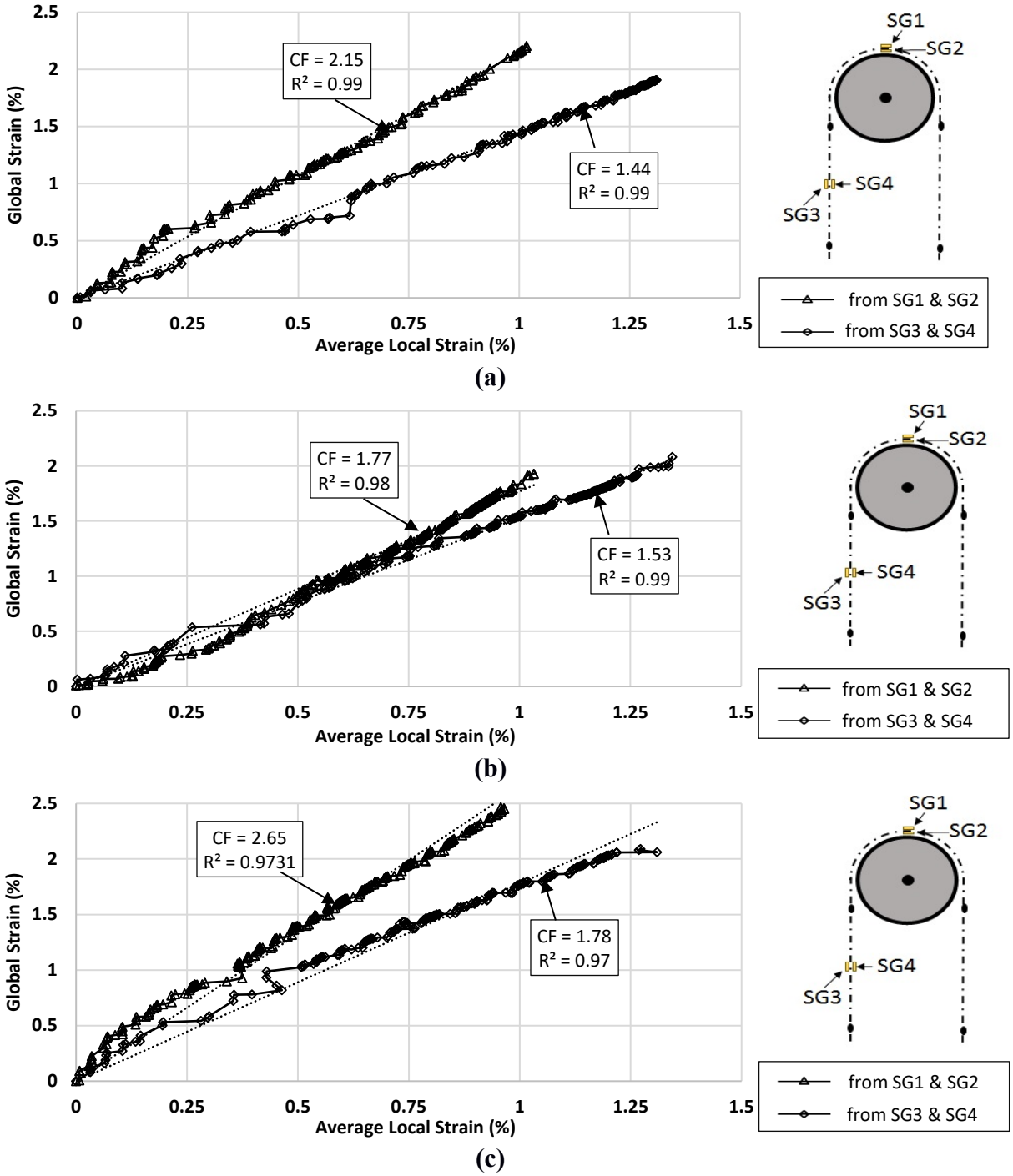

Figure 4. Global strain versus average local strain with the cylinder diameters of: (a) 65 mm; (b) 100 mm; and (c) 160 mm.

where ε_{upper} = the measured local strain from the SG attached on the upper side of the geogrid; ε_{lower} = the measured local strain from the SG attached on the lower side of the geogrid. The calculated CFs from SG1 (ε_{upper}) and SG2 (ε_{lower}) placed on the cylinders with diameters of 65, 100, and 160 mm were 2.15, 1.77, and 2.65, respectively, with an average of 2.19. However, the calculated CFs from SG3 (ε_{upper}) and SG4 (ε_{lower}) using the cylinders with diameters of 65, 100,

and 160 mm were 1.44, 1.53, and 1.78, respectively, with an average of 1.58. Therefore, the friction increased the CF by 39%.

Average Local Strain Ratio. Since the friction is in the opposite direction to the tensile load, the measured strains on the rib on top of the cylinder were lower than those on the vertical rib. Their differences could be calculated and are the indication of the friction effect. Figure 5 shows the differences between the average local strains induced by tension (SG3 and SG4) and those induced by tension, bending, and friction (SG1 and SG2) versus their global strains. The results indicate that the diameter of the cylinder had no effect on the differences between the average local strains. In other words, the cylinders of different diameters had the same friction effect on the measured strains.

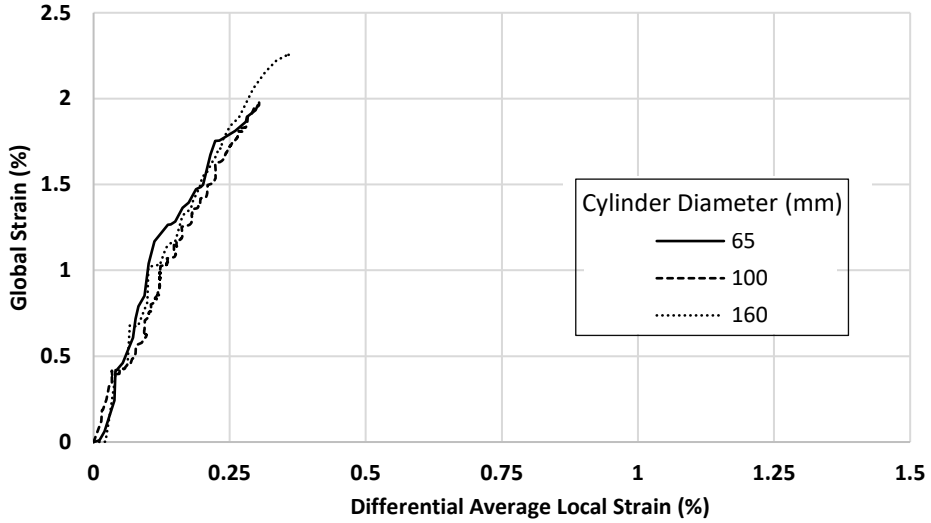

Figure 5. The global strain versus the differential average local strain ratio.

The local strain ratio is the ratio of the average local strain induced by tension only to the average local strain induced by tension, bending, and friction.

$$Local\ Strain\ Ratio = \frac{Average\ Local\ Strain\ (tension\ only)}{Average\ Local\ Strain\ (combined)} \qquad \text{Eq. (3)}$$

Figure 6 shows the average local strain ratio versus the applied load. At a small load (<0.025 kN), the effect of friction was significant. With an increase of the tensile load, this effect became smaller and stable. The result shows that the local strain ratios in the tests with the geogrids wrapped around the cylinders with diameters of 65, 100, and 160 mm were 1.23, 1.22, and 1.38, respectively, with an average of 1.28, after the applied load was higher than 0.025 kN. Figure 6 also shows that regardless of the cylinder diameter, the measured strains induced by tension were approximately 28% higher than the average strains of the upper and lower strains induced by the combination of tension, bending, and friction.

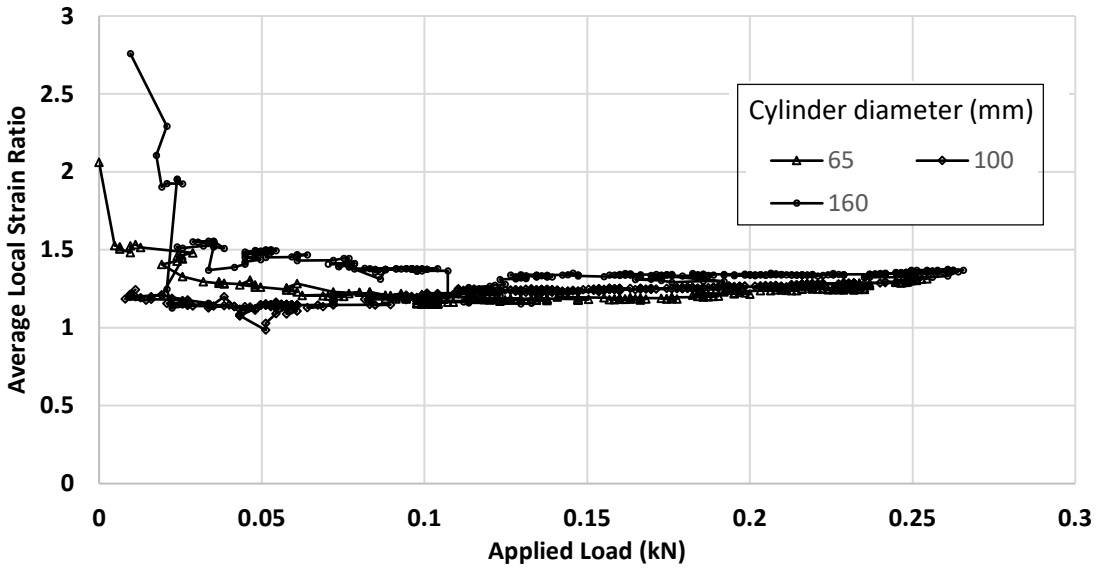

Figure 6. The average local strain ratio versus the applied load.

CONCLUSIONS

The objective of this study was to evaluate the combined effects of tension, bending, and friction on the relationship between local and global strains in the geogrid and on the measured local strains from the upper and lower sides of uniaxial geogrid specimens subjected to tensile force. The following conclusions can be made based on this experimental study:

(1) The effect of friction on the strains in the geogrid could not eliminated by averaging the strains measured by the strain gauges on upper and lower sides of the geogrid.
(2) The global strain in the geogrid induced by tension was higher than that induced by tension, bending, and friction.
(3) The correlation factors (CFs) calculated from the strain gauges subjected to tension, bending, and friction were approximately 39% higher than those calculated from the strain gauges subjected to tension only.
(4) The diameter of the cylinder had a minor effect on the ratio of the average local strain induced by only tension to the average local strain induced by tension, bending, and friction.

ACKNOWLEDGMENT

Tensar International provided the geogrid samples used in this study. The former graduate student, Dr. Jamal Kakrasul, the visiting scholar, Tingyu Wu, and the current graduate students, Saif Jawad, and Mahdi Al-Nadaf in the Department of Civil, Environmental, and Architectural Engineering (CEAE) at the University of Kansas (KU) provided their testing or technical assistance.

REFERENCES

ASTM D-4595 (2011). Standard Test Method for Tensile Properties of Geotextiles by the Wide-Width Strip Method, *American Society for Testing and Materials*, West Conshohocken, Pennsylvania, USA.

Bathurst, R.J., Allen, T.M. and Walters, D.L. (2002). Short-term strain and deformation behavior of geosynthetic walls at working stress conditions. *Geosynthetics International*, 9(5-6): 451-482.

Fannin, R.J. and Hermann, S. (1990). Performance data for a sloped reinforced soil wall. *Canadian Geotechnical Journal*, *27*(5): 676-686.

Han, J. (2015). *Principles and practice of ground improvement*, John Wiley & Sons, Hoboken, New Jersey, USA, ISBN: 978-1-118-25991-7: 432p.

Han, J. and Gabr, M.A. (2002). Numerical analysis of geosynthetic-reinforced and pile-supported earth platforms over soft soil. *Journal of Geotechnical and Geoenvironmental Engineering*, ASCE, 128(1): 44-53.

Hirakawa, D., Kongkitkul, W., Tatsuoka, F. and Uchimura, T. (2003). Time-dependent stress–strain behaviour due to viscous properties of geogrid reinforcement. *Geosynthetics International*, 10(6): 176-199.

Huang, J. and Han, J. (2010). Two-dimensional parametric study of geosynthetic-reinforced column-supported embankments by coupled hydraulic and mechanical modeling. *Computers and Geotechnics*, 37(5): 638-648.

Jiang, Y., Han, J., Parsons, R.L. and Brennan, J.J. (2016). Field instrumentation and evaluation of modular-block MSE walls with secondary geogrid layers. *Journal of Geotechnical and Geoenvironmental Engineering*, ASCE, 142(12): 05016002.

Leshchinsky, D., Imamoglu, B. and Meehan, C.L. (2010). Exhumed geogrid-reinforced retaining wall. *Journal of Geotechnical and Geoenvironmental Engineering,* ASCE, 136(10): 1311-1323.

Maheshwari, P. and Viladkar, M.N. (2009). A mathematical model for beams on geosynthetic reinforced earth beds under strip loading. *Applied Mathematical Modelling*, 33(4): 1803-1814.

Perkins, S.W. and Lapeyre, J.A. (1997). In-isolation strain measurement of geosynthetics in wide-width strip tension test. *Geosynthetics International*, 4(1): 11-32.

Rahmaninezhad, S.M., Han, J., and Kakrasul, J.I. (2018). Behavior of geosynthetic-reinforced retaining walls with wrapped-around and modular block facing subjected to footing loading. Submitted to *Geotextiles and Geomembranes.*

Rahmaninezhad, S.M., Han, J., Kakrasul, J.I., and Weldu, M. (2018). Stress distributions and pullout responses of extensile and inextensible reinforcement in soil using different normal loading methods. *Geotechnical Testing Journal*.

Rahmaninezhad, S.M., Han, J., Weldu, M., and Kakrasul, J.I. (2016). Effects of methods of applying normal stresses in pullout tests on pressure distributions and pullout resistance. *3rd Pan-American Conference on Geosynthetics.* FL. USA.

Rahmaninezhad, S.M., Yasrobi, S.S., Eftekharzadeh, S.F. (2009). Effects of compaction in the subgrade of the reinforced sand backfills with geotextile on bearing capacity. *International Journal of Civil Engineering* 12: 320–328.

Raymond, G.P. (2002). Reinforced ballast behaviour subjected to repeated load. *Geotextiles and Geomembranes*, 20(1): 39-61.

Warren, K.A., Christopher, B. and Howard, I.L. (2010). Geosynthetic strain gage installation procedures and alternative strain measurement methods for roadway applications. *Geosynthetics International*, 17(6): 403-430.

Wayne, M. H., Han, J., and Akins, K. (1998). The design of geosynthetic reinforced foundations. *Design and Construction of Retaining Systems*, *ASCE Geo-Institute Geotechnical Special Publication*, No. 76, edited by John J. Bowders et al., 1-18.

Weldu, M.T., Han, J., Rahmaninezhad, S.M., Parsons, R.L., Kakrasul, J.I. and Jiang, Y. (2016). Effect of aggregate uniformity on pullout resistance of steel strip reinforcement. *Transportation Research Record: Journal of the Transportation Research Board*, 2 (2579): 1-7.

Yasrobi, S.S., Rahmaninezhad, S.M., Eftekharzadeh, S.F. (2009). Large physical modeling to optimize the geometrical conditions of geotextile in reinforced loose sand. *Geotechnical Special Publication* 189: 53-59.